Low absorption chlorinated liquid crystals for infrared applications

Fenglin Peng,[1] Yun-Han Lee,[1] Haiwei Chen, [1] Zhe Li,[2] Andrew E. Bostwick,[2] Robert J. Twieg,[2] and Shin-Tson Wu[1,*]

[1]*College of Optics and Photonics, University of Central Florida, Orlando, Florida 32816, USA*
[2]*Department of Chemistry and Biochemistry, Kent State University, Kent, Ohio 44242, USA*
**swu@creol.ucf.edu*

Abstract: We report a wide nematic range and low absorption loss chlorinated liquid crystal mixture, designated as IR-M2, for mid-wave infrared applications. IR-M2 is quite transparent in the 3.8-5.0 μm window while keeping a high birefringence (Δn~0.194) in the infrared region and a modest dielectric anisotropy. For long-wave infrared applications, we propose another high Δn chlorinated cyanoterphenyl compound.

OCIS codes: (160.3710) Liquid crystals; (260.3060) Infrared.

References and links

1. M. Schadt, "Milestone in the history of field-effect liquid crystal displays and materials," Jpn. J. Appl. Phys. **48**, 03B001 (2009).
2. F. Peng, D. Xu, H. Chen, and S.-T. Wu, "Low voltage polymer network liquid crystal for infrared spatial light modulators," Opt. Express **23**(3), 2361–2368 (2015).
3. P. F. McManamon, T. A. Dorschner, D. L. Corkum, L. J. Friedman, D. S. Hobbs, M. Holz, S. Liberman, H. Q. Nguyen, D. P. Resler, R. C. Sharp, and E. A. Watson, "Optical phased array technology," Proc. IEEE **84**(2), 268–298 (1996).
4. S. T. Wu, J. D. Margerum, H. B. Meng, C. S. Hsu, and L. R. Dalton, "Potential liquid crystal mixtures for CO_2 laser application," Appl. Phys. Lett. **64**(10), 1204–1206 (1994).
5. D. Dolfi, M. Labeyrie, P. Joffre, and J. P. Huignard, "Liquid crystal microwave phase shifter," Electron. Lett. **29**(10), 926–928 (1993).
6. K. C. Lim, J. D. Margerum, and A. M. Lackner, "Liquid crystal millimeter wave electronic phase shifter," Appl. Phys. Lett. **62**(10), 1065–1067 (1993).
7. C.-F. Hsieh, R.-P. Pan, T.-T. Tang, H.-L. Chen, and C.-L. Pan, "Voltage-controlled liquid-crystal terahertz phase shifter and quarter-wave plate," Opt. Lett. **31**(8), 1112–1114 (2006).
8. X. Lin, J. Wu, W. Hu, Z. Zheng, Z. Wu, G. Zhu, F. Xu, B. Jin, and Y. Lu, "Self-polarizing terahertz liquid crystal phase shifter," AIP Adv. **1**(3), 032133 (2011).
9. R. Dąbrowski, P. Kula, and J. Herman, "High birefringence liquid crystals," Crystals **3**(3), 443–482 (2013).
10. S. R. Davis, G. Farca, S. D. Rommel, S. Johnson, and M. H. Anderson, "Liquid crystal waveguides: new devices enabled by >1000 waves of optical phase control," Proc. SPIE **7618**, E1–E14 (2010).
11. S.-T. Wu, "Absorption measurements of liquid crystals in the ultraviolet, visible, and infrared," J. Appl. Phys. **84**(8), 4462–4465 (1998).
12. S.-T. Wu, "Infrared properties of nematic liquid crystals: an overview," Opt. Eng. **26**(2), 120–128 (1987).
13. S.-T. Wu, Q.-H. Wang, M. D. Kempe, and J. A. Kornfield, "Perdeuterated cyanobiphenyl liquid crystals for infrared applications," J. Appl. Phys. **92**(12), 7146–7148 (2002).
14. B. Mistry, *A Handbook of Spectroscopic Data Chemistry: UV, IR, PMR, CNMR and Mass Spectroscopy* (Oxford, 2009).
15. G. W. Gray and A. Mosley, "The synthesis of deuteriated 4-n-alkyl-4-cyanobiphenyls," Mol. Cryst. Liq. Cryst. (Phila. Pa.) **48**(3–4), 233–242 (1978).
16. Y. Chen, H. Xianyu, J. Sun, P. Kula, R. Dabrowski, S. Tripathi, R. J. Twieg, and S.-T. Wu, "Low absorption liquid crystals for mid-wave infrared applications," Opt. Express **19**(11), 10843–10848 (2011).
17. F. Peng, Y. Chen, S.-T. Wu, S. Tripathi, and R. J. Twieg, "Low loss liquid crystals for infrared applications," Liq. Cryst. **41**(11), 1545–1552 (2014).
18. F. Peng, H. Chen, S. Tripathi, R. J. Twieg, and S.-T. Wu, "Fast-response infrared phase modulator based on polymer network liquid crystal," Opt. Mater. Express **5**(2), 265–273 (2015).
19. S.-T. Wu, U. Efron, and L. D. Hess, "Birefringence measurements of liquid crystals," Appl. Opt. **23**(21), 3911–3915 (1984).
20. I. Haller, "Thermodynamic and static properties of liquid crystals," Prog. Solid State Chem. **10**, 103–118 (1975).

#237732 - $15.00 USD Received 10 Apr 2015; revised 30 Apr 2015; accepted 4 May 2015; published 5 May 2015

21. S. T. Wu, U. Efron, and L. D. Hess, "Infrared birefringence of liquid crystals," Appl. Phys. Lett. **44**(11), 1033–1035 (1984).
22. S.-T. Wu, "Birefringence dispersions of liquid crystals," Phys. Rev. A **33**(2), 1270–1274 (1986).
23. S.-T. Wu and C.-S. Wu, "Experimental confirmation of the Osipov-Terentjev theory on the viscosity of nematic liquid crystals," Phys. Rev. A **42**(4), 2219–2227 (1990).

1. Introduction

In addition to amplitude modulation (e.g., displays [1]), liquid crystals (LCs) have also found useful applications for phase modulation [2], such as spatial light modulators for laser beam steering [3], adaptive optics in the mid-wave infrared (MWIR 3~5μm) and long-wave infrared (LWIR 8~12μm) regions [4], as well as phase shifters in the microwave [5,6] and terahertz regions [7–9]. For phase modulation, two types of device structures have been commonly used: (1) deflective beam steering with optical phase array [3] and (2) refractive beam steering with a waveguide structure [10]. For IR applications, besides high birefringence (Δn), low viscosity (γ_1), and large dielectric anisotropy ($\Delta\varepsilon$), low absorption is another critical requirement. Numerous molecular vibration bands exist in the IR region [11]. To steer a high power laser beam in the IR region, the absorption of LC must be minimized because the absorbed light is converted to thermal energy, which in turn heats up the LC material and causes spatial phase non-uniformity [12]. In the extreme case, if the resultant temperature exceeds the LC's clearing point (T_c), then the light modulation capability vanishes completely. Therefore, the LCs employed should be designed to have low absorption and a high T_c.

The molecular vibration bands depend on the spring constant (κ) and reduced mass (μ) of the diatomic group as:

$$\lambda = 2\pi\sqrt{\mu/\kappa}. \tag{1}$$

As the reduced mass increases, the absorption band shifts toward a longer wavelength [13]. In the MWIR region, there exist several vibration bands. For example, the CH, CH_2 and CH_3 absorption bands overlap closely and form a very strong band covering in 3.2~3.7μm [14]. Therefore, three approaches are considered for shifting the vibration bands outside the spectral region of interest: (1) deuteration, (2) fluorination, and (3) chlorination. Substitution of the hydrogens in the alkyl chain and aromatic rings with deuterium doubles the effective mass [15]. As a result, deuteration shifts the CH vibration bands to a longer wavelength by $\sqrt{2}$, i.e. from 3.4μm to 4.8μm, which unfortunately is still in the MWIR region [13]. Therefore, substitution with still heavier atoms is needed. The vibration bands of CF, CF_2 and CF_3 occur at 7~9μm [14]. To suppress the C-H vibration bands in the alkyl chain, some LC compounds and mixtures with a fully fluorinated alkyl chain have been reported. Unfortunately, the vibration bands and overtones of CF, CF_2 and CF_3 also appear in the LWIR and MWIR region separately [16]. While the intensity of the C-F overtones is relatively small, it is still noticeable in the IR region since the required cell gap is relatively thick. In addition, the fluorinated LC mixture only exhibits a nematic phase from 42°C to 51.5°C, which is too narrow for practical applications [17]. Thus, in order to shift the vibration bands and overtones outside the region of interest, we consider the replacement of fluorine with a heavier atom, e.g. chlorine. The C-Cl vibration wavelength occurs in the 12.5 ~15.4μm [14] and therefore the overtone wavelength is now longer than 6μm, which helps to clean up a high transmittance window in the MWIR region. The alkyl chain should be retained to preserve the flexibility and aspect ratio of LC compounds. However, some chlorinated compounds we have reported previously [18] just show monotropic phases and relative high melting points (T_m) as the heavy atom substitution reduce the molecules' flexibility.

In this paper, we describe six chlorinated LC compounds and we have formulated a eutectic mixture with a wide nematic temperature range (–40°C→85°C). The mixture is highly transparent (transmittance >98%) in the MWIR region. Moreover, it shows a relatively high birefringence Δn~0.194 at λ = 4μm, and modest dielectric anisotropy ($\Delta\varepsilon$ = 6.89). For

#237732 - $15.00 USD Received 10 Apr 2015; revised 30 Apr 2015; accepted 4 May 2015; published 5 May 2015

LWIR applications, we prepared a high Δn chlorinated LC with high transmittance at λ = 8~9μm and λ = 10~11μm.

2. Experiment and results

Table 1 lists six chlorinated compounds we have synthesized. In all cases a *p*-terphenyl core unit is employed to obtain high birefringence. The phase transition temperatures were measured by Differential Scanning Calorimetry (DSC, TA instruments Q100). Compounds 1 through 3 only exhibit a monotropic phase and a fairly high melting point. To lower the melting point, we formulated a eutectic mixture (called IR-M1) from these three compounds and it exhibits an enantiotropic phase with T_c = 68°C. Compounds 4 and 5 are chlorinated cyclohexane terphenyls. Although their melting points are relatively high, their nematic temperature ranges are over 100°C. Therefore, to widen the nematic range, we doped 10 wt% of compound 5 into IR-M1 to give a new mixture designated as IR-M2. Compound 4 was not employed here because of its poor solubility, high melting point and large heat of fusion. Remarkably, the melting point of mixture IR-M2 drops to less than −40°C (limited by our DSC) and its clearing point is 85°C. We kept IR-M2 at −40°C for 3 hours and it did not crystalize. Thus, IR-M2 exhibits a wide nematic range including room temperature. Compound 6 is a chlorinated cyano-terphenyl. For the MWIR region, the cyano group should be avoided since it has a very strong absorption peak at ~4.48μm. However, the cyano group elongates the conjugation length and increases the birefringence, which helps to reduce the cell gap and improve the transmittance at LWIR region.

Table 1. Chemical structures and phase transition temperatures of the six chlorinated compounds studied. T_m represents melting point and T_c clearing point.

Compound #.	Chemical structure	T_m (°C)	T_c (°C)
1	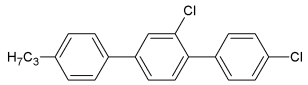	95	68
2	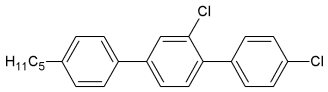	71	65
3	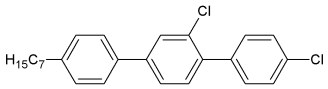	72	67
4	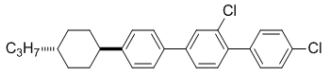	140	257
5	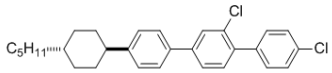	128	253
6	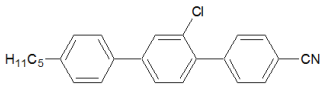	72	98

#237732 - $15.00 USD Received 10 Apr 2015; revised 30 Apr 2015; accepted 4 May 2015; published 5 May 2015

2.1 Temperature dependent birefringence

Birefringence was measured through phase retardation of a homogeneous cell sandwiched between two crossed polarizers [19]. The ITO (indium tin oxide) glass substrates were over-coated with a thin polyimide (PI) layer rubbed in anti-parallel directions to create 2° pre-tilt angle and strong anchoring energy. The cell gap was controlled at ~5μm. The LC cell was mounted in a Linkam LTS 350 Large Area Heating/Freezing Stage controlled by TMS94 Temperature Programmer. A 1 kHz square-wave AC voltage signal was applied to the LC cell. A tunable Argon-ion laser (λ = 457nm, 488nm, and 514nm), a He-Ne laser (λ = 633nm), and a semiconductor laser (λ = 1550nm) were used as light sources. The transmitted light was measured by a photodiode and recorded by a LabVIEW data acquisition system (DAQ, PCI6110). The temperature dependent birefringence of IR-M2 was measured from room temperature (~23°C) to 80°C. Results are plotted in Fig. 1, where black dots represent the measured data and red line is the fitting curve using Haller's semi-empirical equation [20]:

$$\Delta n = \Delta n_0 (1 - T/T_c)^{\beta}, \tag{2}$$

where Δn_0 is the extrapolated birefringence at $T = 0K$ and β is the material constant. Through fitting, we obtained $\Delta n_0 = 0.29$ and $\beta = 0.15$.

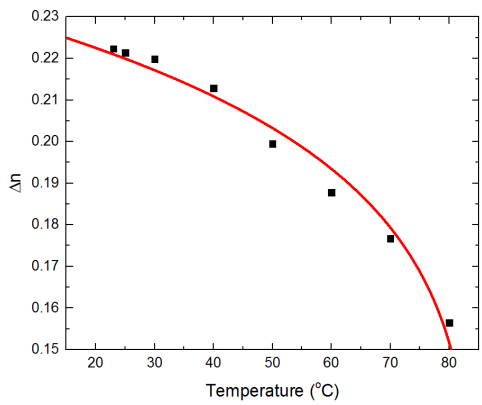

Fig. 1. Temperature dependent birefringence of IR-M2 at λ = 633nm. The black dots are measured data and the red line is a fitting curve with Eq. (2).

2.2 Birefringence dispersion

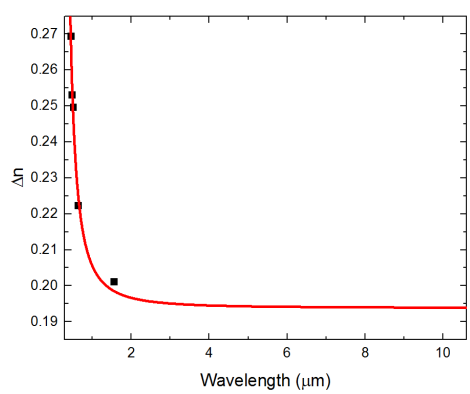

Fig. 2. Birefringence dispersion of IR-M2 at room temperature: the black dots are measured data and the solid line is a fitting with Eq. (3).

#237732 - $15.00 USD Received 10 Apr 2015; revised 30 Apr 2015; accepted 4 May 2015; published 5 May 2015

To determine the birefringence at MWIR region, we measured the dispersion curve as shown in Fig. 2. The red line represents the fitting curve with single-band birefringence dispersion model [21,22]:

$$\Delta n = G\frac{\lambda^2\lambda^{*2}}{\lambda^2-\lambda^{*2}}. \tag{3}$$

where G is a proportionality constant and λ^* is the mean resonance wavelength. Through fitting, we obtained $G = 3.37\mu m^{-2}$ and $\lambda^* = 0.240\mu m$. Based on these parameters, the Δn in the IR region can be extrapolated. As the wavelength increases, Δn decreases sharply and then plateaus in the MWIR region. The birefringence of IR-M2 keeps relatively high (Δn~0.194) in the MWIR region. To achieve 2π phase change at $\lambda = 4\mu m$, the required cell gap is $20.62\mu m$. High Δn enables a thin cell gap to be used for achieving a certain phase change, which in turn leads to fast response time and high transmittance.

2.3 Visco-elastic constant

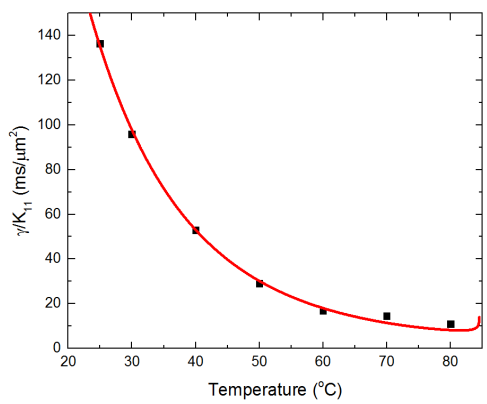

Fig. 3. Temperature dependent visco-elastic coefficients of IR-M2: black dots are measured data and red line is fitting with Eq. (4) at λ = 633nm.

From the response time measurement of the LC cell, we can extract the visco-elastic coefficient (γ_1/K_{11}) [23]. Figure 3 depicts the visco-elatic constant at different temperatures, in which black dots are experimental data and red solid line is the fitting curve with following equation:

$$\frac{\gamma_1}{K_{11}} = A\frac{\exp(E_a/k_B T)}{(1-T/T_c)^{\beta}}. \tag{4}$$

In Eq. (4), A is a proportionality constant, k_B is the Boltzmann constant, E_a is the activation energy, and β is the material constant, which has been obtained through Eq. (2). Through fitting, we obtained E_a = 525meV for IR-M2. The large activation energy results from the heavy chlorine atoms and terphenyl structures. The estimated optical response time is ~800ms. To shorten the response time, a polymer network liquid crystal can be considered and the response time can be improved by 100x, but the tradeoff is incresased operation voltage [18].

2.4 Infrared transmittance

To measure the IR transmittance, we filled IR-M2 to a LC cell with two sodium chloride (NaCl) substrates and measured the transmittance with a Perkin Elmer Spectrum One FTIR Spectrometer. The NaCl substrate is transparent from visible to $14\mu m$ and its refractive index ~1.5 is very close to that of the LC. To suppress the light scattering at room temperature, we

#237732 - $15.00 USD Received 10 Apr 2015; revised 30 Apr 2015; accepted 4 May 2015; published 5 May 2015

spin-coated a thin PI layer (~80nm) on the inner surface of the NaCl substrates and gently rubbed the PI layer. Therefore, the LC molecules are aligned homogeneously. To achieve 2π phase change at $\lambda = 4\mu m$, the required cell gap is $20.62\mu m$. We fabricated an LC cell with a gap of $d = 21\mu m$ and Fig. 4 depicts the measured transmittance of IR-M2 at room temperature from $2\mu m$ to $12\mu m$. In the $3.8\mu m \rightarrow 5\mu m$ region, the transmittance is ~98%. This is because the vibration peaks resulting from C-Cl bonds are shifted to beyond 12.5 μm and the overtone is outside the MWIR window as well. There is a strong absorption peak centered at $3.4\mu m$ resulting from the C-H stretching in the alkyl chain and aromatic rings, which are unavoidable since these C-H bonds are basic elements of organic compounds that exhibit a mesogenic phase. Besides, C-H bond vibrations contribute to the strong absorption at longer wavelength: (1) the C-H deformation in the alkyl chain and C-C skeletal stretching vibration peaks are located at $6\sim8\mu m$; (2) the C-H in-plane deformation vibration peaks are at $8\sim10\mu m$. On the other hand, in the case of a chlorine-substituted ring, the intensity of C-H in-plane bending vibrations is enhanced relative to other absorptions by as much as 3-4x. The absorption peak will degrade the transmittance of the off-resonance region as well. In order to achieve a 2π phase change at LWIR region, e.g. $\lambda = 10.6\mu m$, the required cell gap is ~2x larger than that at MWIR region and the transmittance at $\lambda = 10\sim11\mu m$ is expected to decrease to ~70%. This loss is too large, and other high Δn LC compounds should be considered, as will be discussed later.

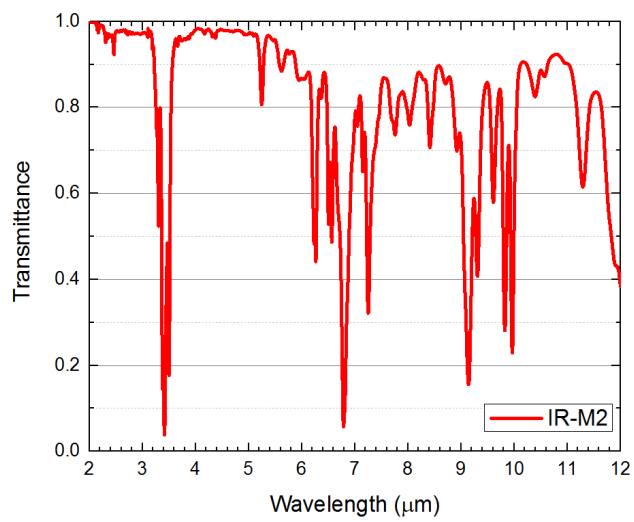

Fig. 4. Measured transmittance spectrum of IR-M2 in the IR region with cell gap $d = 21\mu m$.

2.5 Dielectric anisotropy

In addition to cleaning up the MWIR absorption, the two chloro groups (Table 1, compounds 1-5) also contribute to dielectric anisotropy. To determine the dielectric constants of IR-M2, we measured the capacitance of a homogeneous cell and a homeotropic cell using an HP-4274 multi-frequency LCR meter and found $\Delta\varepsilon = 6.89$ ($\varepsilon_{||} = 10.7$, $\varepsilon_{\perp} = 3.84$) at 23°C and $f = 1$ *kHz*.

2.6 LWIR LC

The transmittance (T) of a liquid crystal layer can be expressed as:

$$T = exp(-\alpha d), \tag{5}$$

where α is the absorption coefficient and d is the cell gap or optical path length. Therefore, to minimize the absorption loss while keeping a required phase change ($\delta = 2\pi d\Delta n/\lambda$) in LWIR

#237732 - $15.00 USD Received 10 Apr 2015; revised 30 Apr 2015; accepted 4 May 2015; published 5 May 2015

region (λ = 8~12μm), two approaches can be considered: 1) To reduce the absorption coefficient α by substituting the C-H in-plane bending vibrations in the aromatic rings, and 2) to employ a high Δn LC to reduce the required cell gap or optical path length. Here, we define a figure-of-merit (*FoM*) to compare the performance of an LC material at a given wavelength:

$$FoM = \Delta n / \alpha. \tag{6}$$

Compound 6 possesses a high birefringence at visible reigon (Δn~0.35 at λ = 633nm) because the combination of the terphenyl core and the cyano group elongate the conjugation length. Based on the birefringence dispersion model, i.e. Equation (3), Δn drops about 10~20% as the wavelength increases from the visible to IR. Here, we suppose Δn~0.29 at λ = 10.6μm and the required cell gap to get a 2π phase change is d = 36.6μm. We also include a commercial LC mixture E7 for comparison. Based on the birefringence dispersion of E7: G = 3.06μm^{-2} and λ^* = 0.250μm, we find Δn~0.19 at λ = 10.6μm. Thus, the required cell gap at this wavelength is 55.8μm. To avoid scattering, we measured the transmittance of compound 6 in the isotropic phase at T~120°C. Figure 5 depicts the measured transmittance of compound 6 and mixture E7 in the LWIR. Compound 6 with higher birefringence and thinner cell gap shows a much higher transmittance than E7 at both λ = 8~9μm and 10~11μm. Some resonance bands of compound 6 are found at λ = 9~10μm because of C-H in-plane vibration resulting from tri-substituted and di-substituted phenyl rings. While the four components in E7 just have di-substituted phenyl rings. Though the CN polar group shows a relatively sharp and strong resonance peak at ~4.48μm, it does not degrade the transmittance in the LWIR region. Similar to IR-M2 for MWIR, we can also formulate eutectic mixtures consisting of homologs of compound 6 for LWIR applications.

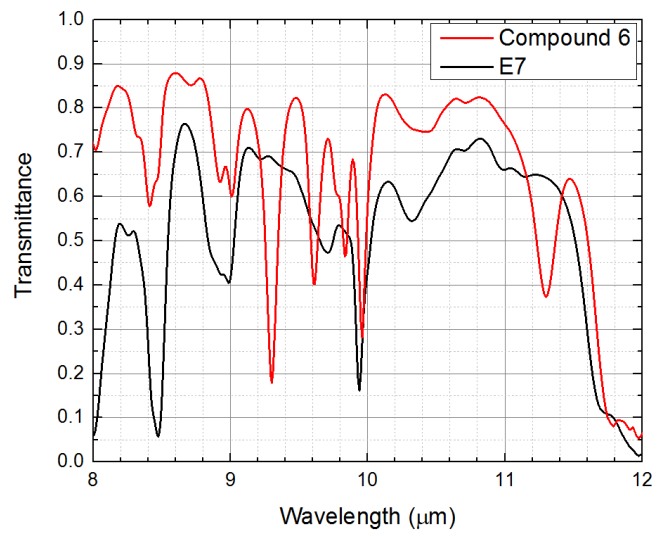

Fig. 5. Measured transmittance spectrum of compound 6 and mixture E7 in the LWIR region. The required cell gaps for compound 6 and mixture E7 are 37μm and 56μm, separately.

3. Conclusion

We have synthesized six chlorinated terphenyl compounds and formulated a eutectic mixture with a broad nematic range (–40°C→85°C). This mixture is quite transparent in the λ = 3.8~5μm widow. To achieve a 2π phase change at λ = 4μm, the required cell gap is ~21μm and the corresponding transmittance is ~98%. To shorten the response time a polymer network liquid crystal can be considered. The response time of ~1ms can be obtained, but the tradeoff is increased operation voltage. In addition, a chlorinated cyanoterphenyl compound shows a

#237732 - $15.00 USD Received 10 Apr 2015; revised 30 Apr 2015; accepted 4 May 2015; published 5 May 2015

relatively high transmittance (>80%) at both λ = 8~9μm and λ = 10~11μm, which has potential applications in the LWIR region.

Acknowledgment

The authors are indebted to Office of Naval Research for the financial support under contract No. N00014-13-1-0096.